

The Discretely-Discontinuous Galerkin Coarse Grid for Domain Decomposition

Essex Edwards* Robert Bridson*

July 8, 2021

Abstract

We present an algebraic method for constructing a highly effective coarse grid correction to accelerate domain decomposition. The coarse problem is constructed from the original matrix and a small set of input vectors that span a low-degree polynomial space, but no further knowledge of meshes or continuous functionals is used. We construct a coarse basis by partitioning the problem into subdomains and using the restriction of each input vector to each subdomain as its own basis function. This basis resembles a Discontinuous Galerkin basis on subdomain-sized elements. Constructing the coarse problem by Galerkin projection, we prove a high-order convergent error bound for the coarse solutions. Used in a two-level symmetric multiplicative overlapping Schwarz preconditioner, the resulting conjugate gradient solver shows optimal scaling. Convergence requires a constant number of iterations, independent of fine problem size, on a range of scalar and vector-valued second-order and fourth-order PDEs.

1 Introduction

Many discretizations of elliptic partial differential equations (PDEs) lead to sparse symmetric positive definite (SPD) linear systems of the form $\mathbf{A}\mathbf{u} = \mathbf{f}$. For large 3D problems, iterative solvers such as preconditioned conjugate gradient (CG) are usually necessary. The condition number often grows quickly as $h \rightarrow 0$, where h is the mesh element size used for discretization: the quality of the preconditioner becomes the crucial factor for efficiency and robustness.

With an optimal preconditioner, the linear system can be solved to desired precision in a time which scales linearly with the problem size. Two popular and related frameworks for potentially optimal preconditioning are multigrid (MG) [6] and domain decomposition (DD) algorithms [14, 17]; we focus on the latter in this paper. The key component we present is a coarse discretization of

* (essex|rbridson)@cs.ubc.ca, University of British Columbia

the PDE, using larger elements of size H , providing the coarse grid correction to accelerate global convergence.

A critical factor in selecting a solver is the question of how much domain knowledge the preconditioner requires. Geometric approaches require the practitioner to re-discretize the PDE at multiple scales, which for irregular domains and/or coefficients may be challenging. In contrast, algebraic approaches work almost entirely with the matrix \mathbf{A} . While algebraic methods may be more difficult to develop, they can provide benefits in both ease of use and in handling irregular problems.

The method we propose here is essentially algebraic, but uses additional discrete information: we ask for a small set of *generating* vectors that span the space of degree p polynomials. We construct a coarse basis by algebraically partitioning the domain into subdomains and using the restriction of each generating vector to each subdomain as its own basis function. The resulting coarse space functions are piecewise-smooth, with jumps at subdomain boundaries. From this basis, we construct a coarse problem by Galerkin projection.

We derive an error bound on the solutions to the coarse problem, and show that it is a high-order accurate convergent coarse grid approximation for a variety of PDEs and discretizations. Convergence requires a limited coarsening factor $[H/h]$ and sufficiently large p . Combined with DD in a Krylov method, we observe the number of required iterations decreases rapidly with p , and has reduced dependence on $[H/h]$, e.g., maintaining optimal scaling in the case $h = H^2$.

For any finite resolution of the fine problem, our coarse bases may or may not be interpreted as discontinuous. However, in the limit as $h \rightarrow 0$ with H fixed, they are equivalent to the bases used in Discontinuous Galerkin (DG) methods [1]. We call our coarse basis functions discretely-discontinuous, giving rise to the name Discretely-Discontinuous Galerkin (DDG) for the approach.

We provide both theoretical and numerical evidence that DDG provides a convenient tool for easily constructing highly effective coarse grid corrections for a wide range of problems, varying over the type of discretization (e.g., classic finite elements or finite differences), the domain (from Cartesian grids to adaptive unstructured meshes), and the underlying PDE (e.g., vector-valued elasticity and fourth-order biharmonic problems).

2 Related Work

Our approach is closely related to the aggregation-based algebraic methods for constructing a coarse basis. For a more thorough review of aggregation techniques in the MG context, we refer the reader to review paper by Stüben [15]. We review the most closely related ideas and the DD setting.

The performance of non-smoothed aggregation, like ours, depends critically on $[H/h]$. The simplest aggregation algorithm produces a piecewise constant coarse space. If $[H/h] = O(1)$, then this preconditioner applied to the Poisson problem has condition number bounded independent of h [12, 13].

For elasticity and higher-order PDEs, a piecewise constant basis is insufficient. Better aggregation techniques have been derived by requiring additional user input: the vectors that span the (near-)nullspace of the PDE [19], e.g., the rigid modes for elasticity and the linear polynomials for biharmonic problems.

These techniques are already optimal, in the sense that the number of iterations is bounded independent of problem size. Improvements to the iteration count can come in the form of constant factor reductions and reduced dependence on $[H/h]$ (or geometric dependencies such as the PDE, domain, coefficients, etc.). Many works present modifications to aggregation-based techniques that improve their performance in these ways.

Despite the optimal scaling of non-smoothed aggregation, when $[H/h]$ is large, the aggregation-based coarse solution is a poor approximation to the actual solution. Galerkin projection finds a solution which is optimal in energy norm, but the near-discontinuities at subdomain boundaries dominate the energy. One way to reduce this dependence on $[H/h]$ is to keep the aggregation basis but apply a non-Galerkin projection, as in over-correction methods that apply a scaling to the Galerkin solution [3, 4]. In practice, this significantly improves the results.

Alternatively, one can work to change the basis. Sala et al. [13] show that the subdomains used for aggregation can be smaller than those used for the DD smoothing step. Following this idea, the associated term in the bound on the condition number reduces geometrically with H . This requires some additional work to come up with the extra partitions, and enlarges the size of the coarse problem.

Another alternative is smoothed aggregation, which smooths the basis functions, thus reducing the steep jumps at subdomain boundaries. For the Poisson problem, this transforms an H/h term in the condition number bound into an H/d term, where d is the smoothing diameter [12]. This keeps the size of the coarse problem the same as basic aggregation, but requires additional work to smooth the basis, and can increase the number of nonzeros in the coarse matrix.

Our method reduces to non-smoothed aggregation if the only generating vector is the constant vector, and our method inherits the upper bounds proven for non-smoothed aggregation. We increase the performance beyond non-smoothed aggregation by using a higher-order basis, which creates to a high-order accurate discretization of the input PDE. By using a p^{th} order coarse basis we reduce the energy at subdomain boundaries from H/h to H^{p+1}/h . We find the added power of higher-order bases greatly reduces the required number of iterations.

Beyond non-smooth aggregation, discontinuous functions have appeared within DD algorithms before. For example, the restricted additive Schwarz method generates discontinuities at subdomain boundaries and has improved performance relative to the equivalent smooth method [7, 10]. When using Discontinuous Galerkin (DG) discretizations, discontinuities are already present in the fine problem. Previous works have developed DD solvers specifically for DG [8, 9], or agglomerated fine DG problems to construct coarse ones [2]. While our approach uses a basis like that of DG methods, it does not require that the fine problem be discretized with DG, but can be interpreted as a discretization of the problem using a DG basis on elements of size H .

3 Preliminaries

The DDG algorithm requires no geometric interpretation or information for implementation (the generating vectors which typically would contain a basis for polynomials in the nodal coordinates are treated as a black box). However, our understanding and analysis is intimately tied to a geometric interpretation, so we frequently refer to the geometric properties for simplicity. For reference, table 1 lists the major symbols used throughout this paper. They are also each defined at first use.

Table 1: Common symbols used throughout the paper.

input, fine grid system	$\mathbf{A}\mathbf{u} = \mathbf{f}$
input, generating basis (tall matrix)	\mathbf{F}
restriction to coarse space	\mathbf{R}_0
restriction to overlapping subdomain $i > 0$	$\tilde{\mathbf{R}}_i$
coarse grid matrix	$\mathbf{A}_0 = \mathbf{R}_0\mathbf{A}\mathbf{R}_0^T$
coarse grid system	$\mathbf{A}_0\mathbf{u}_0 = \mathbf{R}_0\mathbf{f}$
element diameter in fine grid	h
element diameter in coarse grid	H
coarsening factor	$[H/h]$
polynomial degree used in coarse basis	p
subdomain overlap, in geometric distance	δ
subdomain overlap, in algebraic graph distance	Δ
spatial dimension	d

4 The Coarse Grid

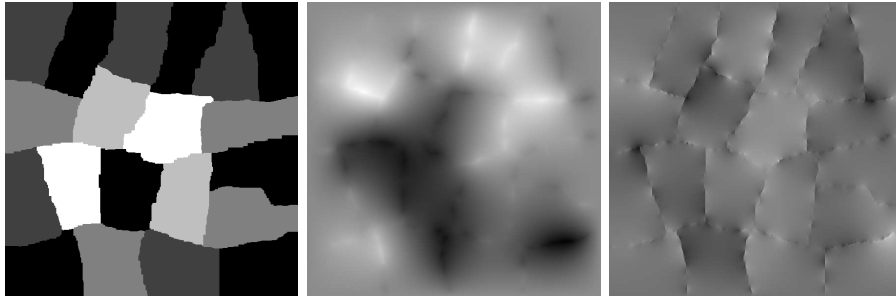


Figure 1: For a simple Poisson problem with random right-hand-side, one-level DD produces a piecewise-smooth error after one iteration. From left to right: partition, error after DD smoothing, x -derivative of error

An effective coarse grid needs to be able to approximate the error left by the one-level DD method. After a single pass of one-level DD, the error is

```

1 % F(i,j) = input basis j evaluated at node i.
2 % Node i is in subdomain partition(i) (zero-based ←
   index).
3 function R0 = basis(F,partition)
4     k = size(F,2);
5     [i,j,s] = find(F);
6     Rt = sparse(i, partition(i)*k+j,s);
7     [Rt,~]=qr(Rt,0); % optional orthogonalization.
8     R0 = Rt';

```

Figure 2: MATLAB code to build the restriction \mathbf{R}_0 from input vectors \mathbf{F} and a partition.

extremely smooth in each subdomain, but not across subdomain boundaries (figure 1). From this structure, we are motivated to use piecewise higher-order polynomials which have a similar piecewise-smooth structure.

Our coarse approximation space consists of piecewise polynomials which are smooth within each subdomain, but have arbitrary jumps at subdomain boundaries. The construction uses several user-supplied vectors, arranged in the columns of \mathbf{F} , that span a degree p polynomial space. For many discretizations, \mathbf{F} can be easily built using the nodal coordinates of the mesh and the constant vector.

To construct the coarse restriction and coarse system matrix, we follow the same Galerkin projection as used in previous aggregation methods (e.g. [19]); the difference is in our choice of \mathbf{F} . The subdomains are built by partitioning the discrete domain into non-overlapping subdomains Ω_i (i.e. subsets of indices) containing approximately $(H/h)^d$ nodes for problems in dimension d . Unless otherwise indicated, all of our examples were partitioned using with a graph-based discrete algorithm from the SCOTCH library [11].

The coarse basis for subdomain i is spanned by the columns of $\phi_i = \mathbf{R}_i^T \mathbf{R}_i \mathbf{F}$, where \mathbf{R}_i is the restriction to the i^{th} partition domain (with no overlap). The final coarse restriction is made by concatenating these basis vectors together as rows in \mathbf{R}_0 . To help with conditioning, we orthogonalize \mathbf{R}_0 , which may be done independently for each subdomain as there is no overlap. Orthogonalization is optional, but the remainder of the paper assumes \mathbf{R}_0 is orthogonal to simplify the analysis. Figure 2 shows simple (albeit inefficient) MATLAB code for this construction. A robust implementation must also detect when ϕ_i is not full rank, and discard columns as necessary.

The coarse matrix \mathbf{A}_0 is constructed by Galerkin projection, $\mathbf{A}_0 = \mathbf{R}_0 \mathbf{A} \mathbf{R}_0^T$, and the coarse approximation to \mathbf{u} (of $\mathbf{A} \mathbf{u} = \mathbf{f}$) is given by $\mathbf{R}_0^T \mathbf{u}_0$ where $\mathbf{A}_0 \mathbf{u}_0 = \mathbf{R}_0 \mathbf{f}$.

The size of \mathbf{A}_0 increases with p , both in rank $\Theta(p^d)$ and in the number of non-zeros $\Theta(p^{2d})$. However, the block sparsity pattern of \mathbf{A}_0 is independent of p .

It has the same sparsity pattern as the subdomain adjacency matrix, but with each non-zero replaced with a small dense block with size dependent on p . This structure allows for efficient numerical linear algebra using dense storage and operations. The optimal choice of p , in terms of total work to solve the problem, will depend on both the problem at hand and details of the implementation, but we generally found $p = 3$, cubic polynomials, is a good default.

5 Coarse Grid Analysis

We show that, under moderate assumptions, the error of the coarse solution is bounded by

$$\|\mathbf{R}_0^T \mathbf{u}_0 - \mathbf{u}\|_{\mathbf{A}} \leq cH^{1+p-q}(1 + [H/h]^{q-1/2})|u|_{\widetilde{W}_\infty^{1+p}(\Omega)} \quad (1)$$

for PDEs of degree $2q$, where c is independent of h and H , and u is the smooth interpretation of \mathbf{u} defined in the next section. When $[H/h] = O(1)$ and $1+p > q$, this error converges at high-order in H . A convergent coarse grid approximation naturally allows the coarse grid correction to capture all components of the error not handled by fine grid smoothing, leading to optimality.

We present two arguments for convergence of the coarse grid. First, we present an argument for FEM discretizations leveraging the extensive theory surrounding FEM and Sobolev norms. Second, we give an alternative argument that depends only on some discrete algebraic properties, which must be shown for each particular discretization.

5.1 Error Bound Using Geometric Properties

Here we restrict our attention to the finite element method.

Let the domain Ω be partitioned into subdomains Ω_i . Let u be in the Sobolev space $W_\infty^q(\Omega)$ (i.e. it should have bounded q^{th} -order weak derivatives) and suppose u is C^∞ in each subdomain. Let $u_h \in W_\infty^q$ be a FEM interpolant of this function on some mesh. We assume that both the subdomains and the mesh elements satisfy all the usual regularity assumptions for meshes with elements of diameter H and h respectively. We represent u_h with a discrete vector \mathbf{u} , assuming a nodal basis, so $\mathbf{u}_i = u(x_i)$. Furthermore, we assume that the FEM interpolant satisfies $\|u\|_{W_2^q} \leq c\|u_h\|_{W_2^q}$, which is true when $\|u\|_{W_2^q} = \|u_h\|_{W_2^q} + O(h)$ and h is smaller than some h_0 .

Let the PDE be given as a symmetric elliptic bilinear form, $a(u, u) = \int_\Omega k[u]^2 d\Omega$, with some linear functional $k[\cdot]$ involving up to q^{th} order derivatives. For example, $k = \nabla$ for the Poisson problem or $k = \nabla^2$ for the biharmonic problem. We assume continuity $a(u, u) \leq c\|u\|_{W_2^q}^2$, where c denotes an arbitrary constant independent of h and H . Discretized with the FEM, $\mathbf{u}^T \mathbf{A} \mathbf{u} = a(u_h, u_h)$.

Each FEM nodal point lies within exactly one subdomain, and has an associated basis function. In some areas, basis functions from multiple subdomains overlap. Let the union of all mesh elements containing these overlapping areas,

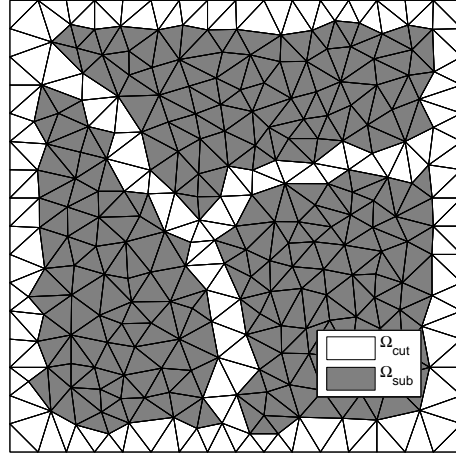


Figure 3: A simple finite element mesh is divided into three subdomains. The elements separating the subdomain interiors from each other and from the boundary conditions are Ω_{cut} . In Ω_{sub} , the error is small because the approximation is good. The error is larger in Ω_{cut} , but the total area is small enough that it does not hinder convergence.

plus any elements touching the boundary of Ω , be Ω_{cut} , and let $\Omega_{sub} = \Omega \setminus \Omega_{cut}$ (figure 3). For the purposes of the proof, we introduce additional bilinear forms $a_{cut}(u, u) = \int_{\Omega_{cut}} k[u]^2 d\Omega$ and a_{sub} defined analogously, along with their discretizations \mathbf{A}_{cut} and \mathbf{A}_{sub} . We note that $a = a_{cut} + a_{sub}$ and $\mathbf{A} = \mathbf{A}_{cut} + \mathbf{A}_{sub}$.

If the mesh and subdomains are sufficiently regular and the FEM basis functions have the usual compact support, then the (d -dimensional) volume $\mu(\Omega_{cut}) \leq c[h/H]$. It is linearly dependent on h because Ω_{cut} is in a band of thickness ch around the subdomain boundaries, and inversely dependent on H because that is the rate at which the total subdomain surface area grows.

As in any Galerkin scheme, the coarse solution $\mathbf{R}_0^T \mathbf{u}_0$ is the minimum error solution in the energy norm over the entire coarse space. Therefore the error is bounded by that of any particular coarse vector, including $\mathbf{v} = \mathbf{R}_0^T \mathbf{R}_0 \mathbf{u}$. Using this and the splitting,

$$\|\mathbf{R}_0^T \mathbf{u}_0 - \mathbf{u}\|_{\mathbf{A}} \leq \|\mathbf{v} - \mathbf{u}\|_{\mathbf{A}} \quad (2)$$

$$= (|\mathbf{v} - \mathbf{u}|_{\mathbf{A}_{sub}}^2 + |\mathbf{v} - \mathbf{u}|_{\mathbf{A}_{cut}}^2)^{1/2} \quad (3)$$

$$\leq |\mathbf{v} - \mathbf{u}|_{\mathbf{A}_{sub}} + |\mathbf{v} - \mathbf{u}|_{\mathbf{A}_{cut}} \quad (4)$$

Before tackling either of these terms, consider what $\mathbf{v} = \mathbf{R}_0^T \mathbf{R}_0 \mathbf{u}$ is. Because \mathbf{R}_0 is orthogonal, $\mathbf{R}_0^T \mathbf{R}_0 \mathbf{u}$ is the l_2 projection of \mathbf{u} onto the coarse space. By construction of the coarse space, \mathbf{v} has a continuous interpretation v that is a degree p polynomial in each subdomain Ω_i . We can find v directly from u by a per-subdomain least-squares approximation of u by a degree p polynomial, minimizing the sum of the squared error at each of the FEM nodal points. Barring

pathological distributions of mesh nodes, v will be a high-order approximation to u , satisfying the same error bounds commonly derived for FEM interpolants on a mesh with elements of size H .

Now, we can bound the discrete error in terms of the geometric functions. We cite the appropriate theorems from Brenner et al. [5] for Sobolev and FEM-interpolant inequalities. Looking first in Ω_{sub} , we find that the coarse polynomials are a high-order approximation:

$$|\mathbf{v} - \mathbf{u}|_{\mathbf{A}_{sub}} \quad \text{error interior to subdomains} \quad (5)$$

$$= |v_h - u_h|_{a_{sub}} \quad \text{discrete and FEM energy are equal} \quad (6)$$

$$\leq c \|v_h - u_h\|_{W_2^q(\Omega_{sub})} \quad \text{continuity assumption} \quad (7)$$

$$\leq c \|v - u\|_{W_2^q(\Omega_{sub})} \quad \text{convergent FEM for sufficiently small } h \quad (8)$$

$$= c \|v - u\|_{\widetilde{W}_2^q(\Omega_{sub})} \quad \text{broken semi-norm defined below} \quad (9)$$

$$\leq c \|v - u\|_{\widetilde{W}_2^q(\Omega)} \quad \text{increasing domain only increases the norm} \quad (10)$$

$$\leq c H^{1+p-q} |u|_{\widetilde{W}_2^{1+p}(\Omega)} \quad \text{Theorem 4.4.20 [5]} \quad (11)$$

$$\leq c H^{1+p-q} |u|_{\widetilde{W}_\infty^{1+p}(\Omega)} \quad \text{2-norm vs. } \infty\text{-norm} \quad (12)$$

Here the broken semi-norm $\widetilde{W}_a^b(Q)$ on domain Q is defined as a sum over subdomains:

$$|u|_{\widetilde{W}_a^b(Q)} = \left(\sum_i |u|_{\widetilde{W}_a^b(\Omega_i \cap Q)}^a \right)^{1/a} \quad (13)$$

This is naturally extended to a maximum over subdomains for $a = \infty$.

Turning to Ω_{cut} , the coarse polynomials are not a high-order approximation in the energy norm, because u is not smooth and v is not even continuous in this region. However, Ω_{cut} is small enough that L^∞ bounds are sufficient.

$$|\mathbf{v} - \mathbf{u}|_{\mathbf{A}_{cut}} \quad \text{error at subdomain boundaries} \quad (14)$$

$$= |v_h - u_h|_{a_{cut}} \quad \text{discrete and FEM energy are equal} \quad (15)$$

$$\leq c \|v_h - u_h\|_{W_2^q(\Omega_{cut})} \quad \text{continuity assumption} \quad (16)$$

$$\leq c h^{-q} \|v_h - u_h\|_{L^2(\Omega_{cut})} \quad \text{Theorem 4.5.12 [5]} \quad (17)$$

$$\leq c h^{-q} \mu(\Omega_{cut})^{1/2} \|v_h - u_h\|_{L^\infty(\Omega_{cut})} \quad \text{2-norm vs. } \infty\text{-norm} \quad (18)$$

$$\leq c h^{-q} [h/H]^{1/2} \|v_h - u_h\|_{L^\infty(\Omega_{cut})} \quad \text{mesh and subdomain regularity} \quad (19)$$

$$\leq c h^{-q} [h/H]^{1/2} \|v - u\|_{L^\infty(\Omega_{cut})} \quad \text{stability of interpolation, 4.4.1 [5]} \quad (20)$$

$$\leq ch^{-q}[h/H]^{1/2}H^{1+p}|u|_{\widetilde{W}_\infty^{1+p}(\Omega_{cut})} \quad \text{Theorem 4.4.20 [5]} \quad (21)$$

$$\leq ch^{-q}[h/H]^{1/2}H^{1+p}|u|_{\widetilde{W}_\infty^{1+p}(\Omega)} \quad \text{increasing domain} \quad (22)$$

$$= cH^{1+p-q}[H/h]^{q-1/2}|u|_{\widetilde{W}_\infty^{1+p}(\Omega)} \quad \text{factor to match eq. (12)} \quad (23)$$

Combining the two bounds 12 and 23 completes the error bound

$$\|\mathbf{R}_0^T \mathbf{u}_0 - \mathbf{u}\|_{\mathbf{A}} \leq cH^{1+p-q}(1 + [H/h]^{q-1/2})|u|_{\widetilde{W}_\infty^{1+p}(\Omega)} \quad (24)$$

5.2 Error Bound Using Algebraic Properties

We can derive a similar bound based purely on algebraic components. As before, let $\mathbf{v} = \mathbf{R}_0^T \mathbf{R}_0 \mathbf{u}$ and $\mathbf{A} = \mathbf{A}_{cut} + \mathbf{A}_{sub}$ be a splitting into symmetric positive semi-definite components. This splitting need not correspond to the FEM definition given earlier. However, we require that $\mathbf{A}_{cut} = \begin{bmatrix} \mathbf{B}_{cut} & \mathbf{0} \\ \mathbf{0} & \mathbf{0} \end{bmatrix}$ with $\mathbf{B}_{cut} \in \mathbb{R}^{m \times m}$ and $m \leq c[h/H]h^{-d}$. This is usually true and plays the role of $\mu(\Omega_{cut})$ from the geometric proof.

We assume that for all $\mathbf{u} \in V$,

$$\|\mathbf{A}_{cut}\|_2 \leq ch^{-2q}, \quad (25)$$

$$\|\mathbf{u}\|_\infty \leq ch^{d/2}\|\mathbf{u}\|_2, \quad (26)$$

$$\|\mathbf{u} - \mathbf{v}\|_{\mathbf{A}_{sub}} \leq cH^{1+p-q}\|\mathbf{u}\|_2, \quad (27)$$

$$\text{and } \|\mathbf{u} - \mathbf{v}\|_\infty \leq cH^{1+p}\|\mathbf{u}\|_\infty. \quad (28)$$

The constants c include the roughness term $|u|_{\widetilde{W}_\infty^{1+p}(\Omega)}$ from the geometric proof. Geometrically speaking, the subspace V must be restricted to functions with bounded roughness.

Showing that these assumptions are true for a particular discretization could exploit geometric properties as in the previous section.

From these assumptions, the convergence argument follows the exact same structure as in the geometric case and we do not repeat it. The final error bound is similar to the above:

$$\|\mathbf{R}_0^T \mathbf{u}_0 - \mathbf{u}\|_{\mathbf{A}} \leq cH^{1+p-q}(1 + [H/h]^{q-1/2})\|\mathbf{u}\|_2. \quad (29)$$

5.3 Proof vs. Practice

The proof and our use of the coarse grid in practice are not entirely consistent with each other. The coarse grid is used to approximate the error after applying one-level DD. For PDEs with smooth coefficients, as $h \rightarrow 0$ with H fixed, the error after one-level DD is piecewise C^∞ as in the proof. For any finite h , it is only an approximation as accurate as the discretization.

In problems with discontinuous coefficients, even as $h \rightarrow 0$, the error after one-level DD is not C^∞ in each subdomain. It has kinks where the coefficients have discontinuities. We tried matching the partition boundaries to the discontinuities, or using a piecewise generating basis \mathbf{F} that matches the discontinuities. We observed optimal scaling even without these strategies, but either strategy significantly accelerated convergence with high-order polynomials.

When we use non-trivial overlap between subdomains, the boundaries of the smooth regions do not line up with the discontinuities in the coarse space. This is easy to resolve by adjusting the coarse subdomains, but this introduces more variation in the coarse subdomains' size and shape. In numerical experiments, better results were obtained by ignoring this inconsistency with the proof and keeping the original subdomain shapes.

The roughness term in the error bound can increase with p , suggesting that the error can actually increase with p . However, because increasing p always grows the coarse vector space, and the Galerkin solve is optimal in that space, increasing p never increases the error.

6 Domain Decomposition

We combine the coarse grid within a standard multiplicative algebraic DD framework.

The DD subdomains begin with the same partition computed for the construction of the coarse basis. From the partition, overlapping subdomains are algebraically constructed by expanding the partition to include nodes within graph distance Δ in the graph defined by \mathbf{A} . The expanded subdomains $\tilde{\Omega}_i$ overlap in geometric bands of size δ . For simple meshes and discretizations, $\delta = (1 + 2\Delta)h$. Unless otherwise indicated, we use minimal overlap $\Delta = 0$.

Let $\tilde{\mathbf{R}}_i$ be the restriction matrix, such that $\mathbf{u}_i = \tilde{\mathbf{R}}_i \mathbf{u}$ is the vector of the elements of \mathbf{u} from subdomain $\tilde{\Omega}_i$, i.e. $\tilde{\mathbf{R}}_i$ is a subset of the rows of the identity matrix. For each subdomain, the local problem uses the matrix $\mathbf{A}_i = \tilde{\mathbf{R}}_i \mathbf{A} \tilde{\mathbf{R}}_i^T$, and we solve these subdomain problems exactly. Given a current approximation \mathbf{u}_k , processing subdomain i updates the approximation to

$$\mathbf{u}_{k+1} = \mathbf{u}_k + \tilde{\mathbf{R}}_i^T \mathbf{A}_i^{-1} \tilde{\mathbf{R}}_i (\mathbf{f} - \mathbf{A} \mathbf{u}_k). \quad (30)$$

Iterating over all subdomains and updating the approximation to \mathbf{u} after each, we arrive at the algorithm for one-level multiplicative overlapping Schwarz.

To build a two-level method, we multiplicatively combine one pass of one-level Schwarz as a pre-smoother, the coarse problem solution, and another pass through the subdomains as a post-smoother. The post-smoother is done in reverse order, making the entire operation symmetric and usable with CG.

We give some experimental results with a three-level method operating in a V-cycle. We construct the three-level problem by taking the two-level algorithm and applying it again to the coarse matrix \mathbf{A}_0 to make an even coarser matrix \mathbf{A}_1 . To do this, we need a coarsened version of the generating vectors, which are simply $\mathbf{F}_0 = \mathbf{R}_0 \mathbf{F}$. The coarsened coarse problem is equivalent to directly

coarsening the original problem with larger subdomains. We keep the ratio between physical element sizes in adjacent levels the same (i.e. $h/H_0 = H_0/H_1$). The algebraic overlap Δ used for smoothing is also the same at all levels.

6.1 Condition Number

For several special cases, our approach reduces to previously published aggregation approaches. For the Poisson problem using $p = 0$, Sala [12] showed that the additive variant of the preconditioner has condition number bounded by $O(1 + [H/h])$. For elasticity and biharmonic problems with $p = 1$, our approach is essentially a non-smoothed two-level variant of the multigrid method described by Vaněk et al. [19]. Their coarse grid uses the zero-energy modes, which are $p = 1$ for biharmonic and a subset of $p = 1$ for elasticity. They later prove optimal convergence, but only for the Poisson problem [18]. We do not have a condition number bound showing the dependence on p and q . However, increasing p beyond the low-order choices in the literature increases the dimension of the coarse space, which does not have a negative effect on convergence – it can only increase the rate of convergence.

7 Numerical Experiments

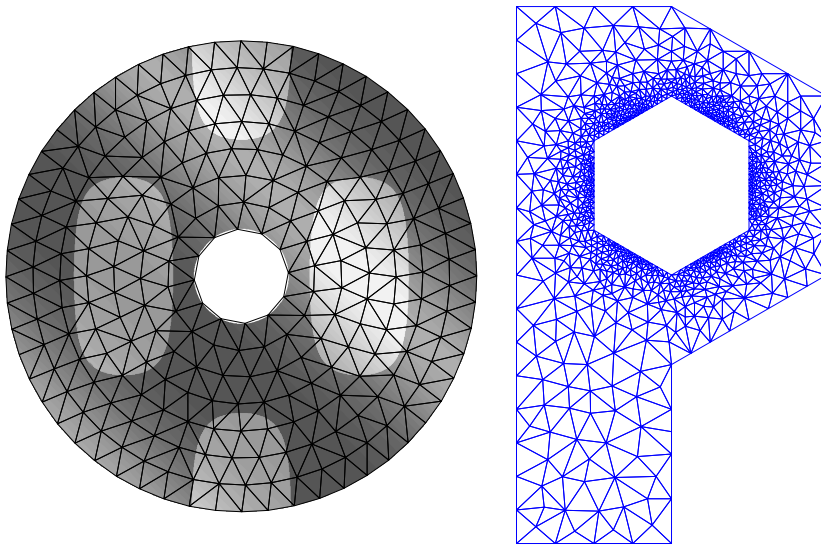


Figure 4: Left: sample annulus mesh used for Poisson problems B,C,D, with shading showing $S + 10J$. Right: sample adaptive mesh used for elasticity problem E.

We demonstrate the performance of our coarse grid and DD as a preconditioner for CG on a variety of PDEs and discretizations. Unless otherwise

noted, all problems are solved to a 10^{-9} reduction in residual after the first application of the preconditioner. The right-hand-side vector \mathbf{f} is a random Gaussian-distributed vector, and the initial guess for \mathbf{u} is $\mathbf{0}$. For the sake of easier reporting, we consider all problems with uniform meshes to be scaled such that $\text{rank}(\mathbf{A}) = n = h^{-d}$, where d is the spatial dimension. Consequently, H^{-d} is the number of subdomains.

The graph of the logarithm of the residual vs. the iteration count is typically very straight. Therefore we measure not just the integer iteration on which the residual is first smaller than the tolerance, but also the fractional iteration count at which the linear interpolation of this graph meets the tolerance. We found this reveals a lot of otherwise hidden detail, and this is shown in some figures. When CG takes more than 1000 iterations, we stop the solve and report iteration bounds based on condition number estimates derived from the Lanczos coefficients computed during CG. For converged problems, these bounds agreed very well with actual iteration counts.

Scaling with h and H are already well explored in the existing aggregation-based literature. Our approach does not perform significantly differently along these axes, so we concentrate on the dependence on p and the novel scaling regimes that our approach can handle.

We use the following problems:

- (A) *Poisson 3D*. $\nabla \cdot \nabla u = f$ discretized on an $m \times m \times m$ regular grid with a 7-point finite difference stencil. One face of the cube has a Dirichlet boundary condition and the remainder are Neumann. For this problem, we partition using recursive inertial partitioning [16] so that the matrix need never be explicitly constructed. The first partition uses a randomly-oriented plane to ensure irregularly shaped subdomains.
- (B) *Smooth Poisson*. $\nabla \cdot S \nabla u = f$ discretized with piecewise linear finite elements on a 2D unstructured triangle mesh of a circular annulus with outer radius 5 times the inner radius. Both inner and outer boundaries use Dirichlet conditions. The scalar function $S = \exp(1 + \sin(\pi(x + y)))$ is smooth. See figure 4.
- (C) *Non-Smooth Poisson*. $\nabla \cdot D \nabla u = f$ discretized as above, but with discontinuous $D = S + 100J$ where $J = \mathbf{H}(0.25 + \cos(\pi x) \cos(2\pi y))$ with Heaviside step function H . J is an indicator function for two ‘materials’ in the problem. We used algebraic partitions that do not conform to the material boundaries, but we use generating vectors \mathbf{F} that are piecewise polynomial with respect to the material domains. This doubles the number of columns in \mathbf{F} , but only subdomains that include the material boundary end up with additional coarse basis functions, so \mathbf{A}_0 is only marginally larger. In practice, we observe optimal scaling even without this extra work and it makes no difference with the piecewise constant basis. However, with the piecewise cubic basis, this material-aware \mathbf{F} reduces the iteration count by nearly one half.

- (D) *High-Order Poisson.* $\nabla \cdot \nabla$ discretized as in B and C, but with continuous piecewise cubic finite elements.
- (E) *Elasticity.* $(\nabla \cdot \nabla + \nabla \nabla \cdot)u = f$ with Dirichlet boundary conditions, with vector u . This is discretized on a spatially-adaptive unstructured 2D triangle mesh (figure 4) with piecewise linear FEM. For the generating vectors \mathbf{F} , we take the degree p polynomials in each component of u .
- (F) *Biharmonic.* $\nabla^4 u = f$ on a regular $m \times m$ 2D grid discretized with a 13 point finite difference stencil. All boundaries have homogenous Dirichlet and Neumann conditions. This problem uses an algebraic overlap $\Delta = 1$, since performance is quite poor with $\Delta = 0$. Also this problem is solved only to 10^{-6} reduction in residual, as the fine discretizations are very poorly conditioned causing CG to break down before reaching 10^{-9} as used in the above.

Table 2 summarizes the results for solving these problems at different h , H , and polynomial coarse spaces from piecewise constant P_0 to cubic P_3 . With fixed $[H/h]$, we observe near constant iteration counts, independent of the problem size, when using the two-level algorithm. Part of the increase in iteration count can be attributed to degrading partition quality with the algebraic partitioner. Experiments (not shown) with more structured partitioning of the structured meshes showed less variation in iteration counts. The three-level V-cycle does not perform nearly as well, but still appears to be sub-logarithmic in n .

Table 3 shows the wall-clock time spent on setup (excluding partitioning) and solution of some problems from table 2. The 2D problems were solved with a MATLAB implementation that solved each subdomain problem with the “backslash” operator on each iteration, but stored a factorization of the coarse grid. The 3D problems were solved with a parallel C++ implementation that solved the subdomains with successive over-relaxation, and solved the coarse grid with conjugate gradient, preconditioned with incomplete Cholesky. Both implementations ran on a 32-core Intel Xeon E5-2690 with 256GB of RAM. In all cases, the bulk of the runtime is spent on the subdomain solves, despite the use of poorly-scaling solvers for the coarse problem. Furthermore, the runtime scales approximately linearly with problem size, as desired.

To directly explore the value in using higher-order coarse bases, we solve a 1000×1000 biharmonic problem with varying p , a large coarsening factor $[H/h] = 125$, and $\Delta = 2$. The large coarsening factor is desirable for efficient parallel implementations, but significantly reduces the accuracy of the low-order coarse grids. As shown in figure 5, we observe the number of iterations decreases rapidly with increasing p .

Note that increasing p increases the size of \mathbf{A}_0 , so there are diminishing returns with large p . Nonetheless, significant reductions in problem size are achieved for all p . The least reduction, with $p = 10$, is $\text{rank}(\mathbf{A}_0) = (1/284) \cdot \text{rank}(\mathbf{A})$. A similar effect occurs in aggregation techniques when the aggregation subdomains are smaller than the subdomains used in smoothing. We compare

Table 2: Iterations of CG to solve various problems in n variables. P_0 , i.e. non-smoothed aggregation, is not expected to achieve optimal scaling for ∇^4 ; the P_0 column is included for comparison only. Problems marked “ \times ” are too small to use the three-level solver - the coarsest partition would be a single subdomain.

$n^{1/d}$	Two-Level								Three-Level			
	$H/h=10$				$H/h=20$				$H/h=10$			
	P_0	P_1	P_2	P_3	P_0	P_1	P_2	P_3	P_1	P_2	P_3	
$\nabla \cdot \nabla$ 3D	40	36	20	15	12	35	23	18	15	\times	\times	\times
	80	41	20	16	13	51	28	21	18	\times	\times	\times
	160	44	21	16	13	61	30	23	19	39	29	23
	320	44	21	16	14	63	30	23	19	43	32	26
	640	46	22	16	14	65	31	23	19	48	35	34
$\nabla \cdot S\nabla$	200	41	19	14	11	51	25	20	15	26	23	19
	400	44	19	14	11	60	26	19	16	40	29	24
	800	48	20	15	12	64	27	20	17	43	31	23
	1600	52	20	15	12	68	28	22	17	45	32	25
	3200	52	21	16	13	71	29	22	17	45	32	25
$\nabla \cdot D\nabla$	200	43	19	15	12	56	27	22	16	32	27	25
	400	46	20	15	13	64	28	22	19	42	28	24
	800	48	21	16	13	67	31	23	18	43	31	25
	1600	52	21	17	14	69	33	23	20	47	34	26
	3200	58	24	17	13	69	31	24	19	49	35	27
$\nabla^2 P_3$ -FEM	200	47	22	17	14	58	29	21	17	33	24	21
	400	53	22	17	14	68	29	22	19	44	34	25
	800	53	24	17	14	73	31	23	19	47	33	26
	1600	56	23	19	15	75	32	25	19	49	35	28
	3200	67	24	18	15	83	32	24	20	50	36	28
Elasticity	200	72	29	21	19	83	40	32	25	\times	\times	\times
	400	81	29	24	18	96	41	30	25	47	37	30
	800	82	33	23	20	104	42	31	26	67	48	39
	1600	76	32	24	20	107	44	33	27	69	51	36
	3200	76	33	27	23	108	47	36	29	71	50	40
∇^4	200	698	62	20	12	600	154	44	24	119	40	22
	400	2900	68	21	12	3500	188	53	27	376	112	37
	800	5700	77	25	15	6900	184	55	32	961	156	51
	1600	9500	99	31	15	11000	246	70	30	2100	169	58

to this approach by using $p = 1$ but aggregating on smaller subdomains. The high- p basis significantly outperforms this approach (figure 5).

Our error bound does not strictly require that $[H/h] = O(1)$ in order to produce a convergent coarse grid, and accompanying optimal preconditioner. For Poisson ($q = 1$) using a piecewise linear coarse basis ($p = 1$) and substituting

Table 3: Execution times for the middle column of table 2 (two-level scheme with $H/h=20$). Each entry shows the wall-clock time in seconds and the percent of total runtime spent on coarse grid setup and solution. Problems marked “ \times ” did not converge within 1000 iterations.

	$n^{1/d}$	P_0	P_1	P_2	P_3
$\nabla \cdot \nabla$ 3D	40	79 (0%)	55 (0%)	42 (0%)	32 (1%)
	80	152 (1%)	87 (1%)	64 (2%)	53 (3%)
	160	481 (2%)	238 (4%)	186 (6%)	160 (11%)
	320	1207 (3%)	614 (8%)	525 (15%)	497 (27%)
	640	7053 (5%)	3785 (16%)	3140 (25%)	3563 (43%)
$\nabla \cdot S\nabla$	200	12 (2%)	5 (2%)	4 (3%)	3 (7%)
	400	48 (1%)	22 (2%)	17 (4%)	15 (8%)
	800	246 (1%)	108 (2%)	87 (4%)	72 (9%)
	1600	1283 (1%)	572 (2%)	423 (4%)	358 (9%)
	3200	6491 (0%)	2767 (2%)	2107 (4%)	1711 (9%)
$\nabla \cdot D\nabla$	200	11 (1%)	5 (2%)	4 (5%)	4 (11%)
	400	51 (1%)	22 (2%)	18 (5%)	16 (11%)
	800	227 (1%)	100 (2%)	84 (6%)	67 (13%)
	1600	1051 (1%)	496 (2%)	362 (6%)	320 (12%)
	3200	7170 (0%)	3006 (2%)	2254 (4%)	1896 (10%)
$\nabla^2 P_3$ -FEM	200	18 (1%)	9 (1%)	6 (4%)	6 (5%)
	400	92 (0%)	43 (1%)	32 (3%)	27 (6%)
	800	440 (0%)	190 (1%)	149 (3%)	121 (7%)
	1600	1902 (0%)	853 (1%)	635 (4%)	498 (8%)
	3200	10223 (0%)	4123 (1%)	3183 (3%)	2706 (7%)
Elasticity	200	30 (0%)	15 (1%)	11 (3%)	9 (6%)
	400	147 (0%)	60 (1%)	46 (3%)	42 (7%)
	800	644 (0%)	263 (1%)	207 (3%)	172 (7%)
	1600	2778 (0%)	1160 (1%)	883 (4%)	727 (8%)
	3200	14958 (0%)	6202 (1%)	5017 (3%)	4625 (6%)
∇^4	200	198 (0%)	57 (1%)	17 (1%)	11 (3%)
	400	\times	321 (0%)	86 (1%)	45 (4%)
	800	\times	1565 (0%)	484 (2%)	225 (5%)
	1600	\times	7900 (1%)	2171 (2%)	1012 (5%)

the relationship $h = H^2$, we arrive at the convergent bound

$$\|\mathbf{R}_0^T \mathbf{u}_0 - \mathbf{u}\|_{\mathbf{A}} \leq cH^{1/2} |u|_{\widetilde{W}_\infty^2(\Omega)}. \quad (31)$$

Figure 6 shows the Poisson problem B with these parameters. Each subdomain has a number of nodes equal to the number of subdomains, so the coarse matrix and the subdomain matrices are a similar size, which is an interesting point in the design space. As in all overlapping DD methods, the smoother is very sensi-

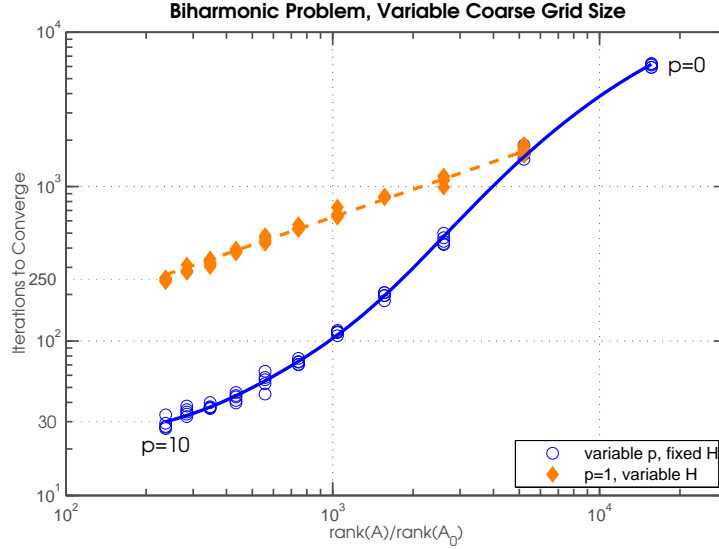


Figure 5: The number of required iterations decreases rapidly with polynomial degree used in the coarse basis (parameters: $h^{-1} = 1000$, $[H/h] = 125$, $\Delta = 2$). For comparison, when using $p = 1$ but aggregating using smaller subdomains, the iteration count is much higher for the same number of coarse variables.

tive to H/δ . To keep it approximately constant, we set $\Delta = \lfloor H/4h \rfloor$. The minor saw-tooth pattern in the graph comes directly from the remaining variation in H/δ . With higher polynomial degrees, $h = H^s$ for higher powers of s would be possible.

8 Discussion

There are a number of outstanding questions raised by this work. We've shown a bound on the error of the coarse grid, dependent on p and the smoothness of the solution. Ideally, we would have a thorough understanding of the relationship between all of the parameters (H , h , p , δ , and q) and the condition number or number of iterations to converge. We leave closing this gap in the analysis for future work.

On the more practical side, the generating vectors \mathbf{F} are not difficult to supply, but it would be more convenient to construct similar high-order coarse grids directly from \mathbf{A} . Also, our approach still has the same undesirable dependency on $[H/h]$ that is present in many algebraic approach, but is not present in geometric methods. Following the connection between the coarse basis and DG, we have done some preliminary work on algebraically constructing a DG-like discretization that is independent of $[H/h]$, but with mixed success.

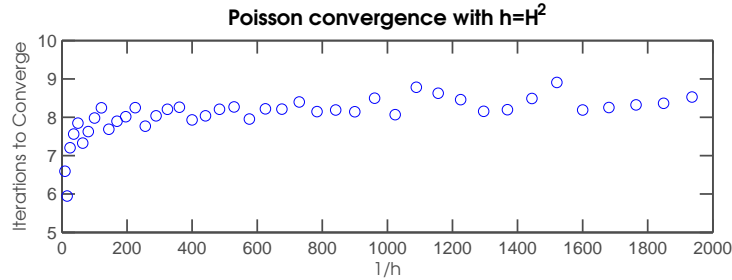


Figure 6: Our grid is convergent and has approximately h -independent convergence, even when $[H/h]$ is not fixed. Parameters: $h = H^2$, $2\delta \approx H$, $p = 1$.

9 Conclusion

We have presented an algebraic coarse grid construction that produces a convergent rediscretization of the PDE for a wide variety of PDEs. It works for both scalar- and vector-valued problems, both second- and fourth-order PDEs, and both smooth and discontinuous coefficients. The high-order DG-like coarse basis is easy to construct algebraically, and Galerkin projection generates a high-order convergent coarse rediscretization of the input problem. Combined with DD and CG, we observe convergence in a number of iterations nearly independent of problem size. Furthermore, increasing the polynomial degree rapidly reduces the number of required iterations: the fastest solves used high-degree polynomials.

References

- [1] D. ARNOLD, F. BREZZI, B. COCKBURN, AND L. D. MARINI, *Unified analysis of discontinuous galerkin methods for elliptic problems*, Siam J. Numer. Anal., 39 (2002), pp. 1749–1779.
- [2] F. BASSI, L. BOTTI, A. COLOMBO, D. A. D. PIETRO, AND P. TESINI, *On the flexibility of agglomeration based physical space discontinuous galerkin discretizations*, Journal of Computational Physics, 231 (2012), pp. 45 – 65.
- [3] R. BLAHETA, *A multilevel method with overcorrection by aggregation for solving discrete elliptic problems*, J. Comput. Appl. Math., 24 (1988), pp. 227–239.
- [4] D. BRAESS, *Towards algebraic multigrid for elliptic problems of second order*, Computing, 55 (1995), pp. 379–393.
- [5] S. C. BRENNER AND R. SCOTT, *The mathematical theory of finite element methods, third edition*, vol. 15, Springer, 2008.

- [6] W. L. BRIGGS, S. F. MCCORMICK, ET AL., *A multigrid tutorial*, vol. 72, Siam, 2000.
- [7] X. CHUAN CAI AND M. SARKIS, *A restricted additive Schwarz preconditioner for general sparse linear systems*, SIAM J. Sci. Comput, 21 (1999), pp. 792–797.
- [8] E. G. D. DO CARMO AND A. V. C. DUARTE, *A discontinuous finite-element based domain decomposition method*, Comput. Meth. Appl. Mech. Engrg., 190 (2000), pp. 825–843.
- [9] M. DRYJA, J. GALVIS, AND M. SARKIS, *Bddc methods for discontinuous galerkin discretization of elliptic problems*, Journal of Complexity, 23 (2007), pp. 715–739.
- [10] E. EFSTATHIOU AND M. GANDER, *Why restricted additive Schwarz converges faster than additive Schwarz*, BIT Numerical Mathematics, 43 (2003), pp. 945–959.
- [11] F. PELLEGRINI AND J. ROMAN, *Scotch: A software package for static mapping by dual recursive bipartitioning of process and architecture graphs*, in High-Performance Computing and Networking, vol. 1067, Springer, 1996, pp. 493–498.
- [12] M. SALA, *Analysis of two-level domain decomposition preconditioners based on aggregation*, ESAIM: Mathematical Modelling and Numerical Analysis, 38 (2004), pp. 765–780.
- [13] M. SALA, J. N. SHADID, AND R. S. TUMINARO, *An improved convergence bound for aggregation-based domain decomposition preconditioners*, SIAM J. Matrix Anal. Appl., 27 (2005), pp. 744–756.
- [14] B. SMITH, P. BJØRSTAD, AND W. GROPP, *Domain Decomposition - Parallel Multilevel Methods for Elliptic Partial Differential Equations*, Cambridge University Press, 1996.
- [15] K. STÜBEN, *A review of algebraic multigrid*, Journal of Computational and Applied Mathematics, 128 (2001), pp. 281 – 309. Numerical Analysis 2000. Vol. VII: Partial Differential Equations.
- [16] V. TAYLOR AND B. NOUR-OMID, *A study of the factorization fill-in for a parallel implementation of the finite element method*, Int. J. Numer. Meth. Engng, 37 (1994), pp. 3809–3823.
- [17] A. TOSELLI AND O. WIDLUND, *Domain Decomposition Methods - Algorithms and Theory*, vol. 34 of Springer Series in Computational Mathematics, Springer, 2004.
- [18] P. VANĚK, M. BREZINA, J. MANDEL, ET AL., *Convergence of algebraic multigrid based on smoothed aggregation*, Numerische Mathematik, 88 (2001), pp. 559–579.

- [19] P. VANĚK, J. MANDEL, AND M. BREZINA, *Algebraic multigrid by smoothed aggregation for second and fourth order elliptic problems*, Computing, 56 (1996), pp. 179–196.